Preprints of the 21st IFAC World Congress (Virtual)
Berlin, Germany, July 12-17, 2020

Dual-stage Soft Landing for a Pick-and-place Manipulator ⋆

Adam Polák * **Martin Hromčík** ** **Ondřej Novák** ***
Zdeněk Hurák ****

* *Faculty of Electrical Engineering, Czech Technical University in Prague (e-mail: adam.polakk@gmail.com).*
** *Faculty of Electrical Engineering, Czech Technical University in Prague (e-mail: xhromcik@fel.cvut.cz)*
*** *EZconn technologies CZ s.r.o. (e-mail: ondrej.novak@ezconn.cz)*
**** *Faculty of Electrical Engineering, Czech Technical University in Prague (e-mail: hurak@fel.cvut.cz)*

Abstract: In this paper we document a systematic solution to a particular motion control problem called soft landing encountered in the design of pick-and-place machines for the semiconductor industry. The problem has already been studied for a single actuator, and a solution for the case of voice-coil motors has already been implemented in commercial drivers. Here we investigate a more complex setup consisting of two translation stages, which make the problem over-actuated; furthermore, the inner stage (actuated by a voice coil motor) is preloaded with a weight- compensating spring. Our systematic approach is based on the concept of reaction force observer. Its functionality is demonstrated using numerical simulations and laboratory experiments. We compare the proposed method with a baseline solution based on a simple extension of an existing method. A related Simulink model and Matlab scripts are available for free download to help reproduce the results.

Keywords: soft landing, dual-stage, motion control, force control, reaction force observer, voice coil motor.

1. INTRODUCTION

1.1 Motivation

In this paper we document a systematic solution to a particular motion control problem called *soft landing*. The task is to drive an end effector (tool) as fast as possible to physical contact with another object and exert a specified force on it. Neither during the impact nor the subsequent contact can the force exceed some given limits. The problem is encountered when designing a motion control system for pick-and-place machines used in semiconductor industry—the tool carrying a component travels over a relatively large distance (at least several millimeters but often even a few centimeters) until it reaches a silicon wafer, against which it pushes the component with a specified force while it is being soldered to the wafer. After soldering is done, the tool retracts, picks another component and the mission is repeated. Minimizing cycle time is desirable. Here we investigate a more complex setup consisting of two translation stages, which make the problem over-actuated. Furthermore, the inner stage (actuated by the voice coil motor) is preloaded with a weight-compensating spring. In this setup, the application of existing techniques is not straightforward and modification is needed. We present two solution methods: one based on an extension of one existing soft landing approach, the other based on the concept of reaction force observer.

⋆ Sponsored by the Ministry of Industry and Trade of the Czech Republic within project FV20403 (TRIO II).

1.2 State of the art

Although the topic of force control has found its way to robotics textbooks, here we face the need to effectively switch between position/velocity control and force control. A textbook solution to this problem seems to be the framework of hybrid position/force control introduced by Raibert and Craig (1981), within which the force control loop is closed around a position/velocity loop. It is known, however, from Katsura et al. (2006) that if force sensors are used to get the measurement for the feedback, the resulting behavior might be oscillatory due to often limited bandwidth of force sensors. Inspired by Peng et al. (2010), we wanted to get along without force sensors. Provided that initially, an end effector is at some distance from the surface to be contacted, an intuitive procedure starts within a position control mode, that is, the manipulator ramps up the speed until it reaches the maximum value, then it continues at this maximum speed and ramps down at a given short distance from the surface. It then continues slowly in the velocity mode while continuously detecting if there was a hit. Once a hit is detected, the system switches to a force mode, ramping up the force to the reference

value. In case of linear dc (voice coil) motors, this intuitive solution was patented [1] .

A systematic framework fitted to the described problem seems to be the one based on the reaction force observer (RFOB) introduced in the 1990s by Murakami et al. (1993). Some new results on the adaptation of RFOB have been recently proposed by Sariyildiz and Ohnishi (2015). In this paper we adopt this approach and fit it into the dual-stage framework.

A dual-stage configuration has been exploited in some motion control applications such as read-write heads for hard disk drives, for example, see Clayton et al. (2014) or inertial stabilization, see Řezáč and Hurák (2013). In such applications, the motivation for this kind of overactuation is to get an extra range of motion while at the same time keep the benefits of high-performance (accuracy, bandwidth, linearity) of short-range actuators. In addition to that, here we also need to incorporate the impact/contact force control aspects into the structure of the controller. To the best of our knowledge, no systematic procedure for soft landing adapted to the dual-stage configuration has been published.

1.3 Outline of the paper

In the next Section 2 we describe the laboratory setup. In Section 3 we present a mathematical model. Then, in Section 4 we document the control design routines. We verify the designed controllers in Section 5 by means of simulations and in Section 6 through laboratory experiments. Readers can also download both the Simulink model and the related Matlab script to reproduce the design and the simulations.

2. EXPERIMENTAL MOTION CONTROL SETUP

The laboratory platform design is based on an industrial robot for die-attach soldering. It consists of two linear drive stages which represent the robot motion in the vertical axis.

The first linear drive, later referenced as the primary stage, is composed of a permanent magnet synchronous motor (PMSM) and a ball screw linear drive connected via a shaft coupler. The PMSM is manufactured by the company ESR Pollmeier GmbH and it is controlled by a control unit by the same manufacturer. The linear drive has a range of 16 cm and the incremental position sensor has a resolution of 1 µm.

The secondary linear stage is a linear voice coil motor (VC) SLA25 by the company SMAC. It has a range of 1 cm and the incremental position sensor with a resolution of 1 µm as well. For the reference solution to the soft landing problem, the driver by the manufacturer SMAC is used. Because of its inconvenience for experimental purposes, we have developed a custom driver electronics for the voice coil motor, which we use in the proposed control method.

The whole experimental setup is depicted in figure 1. The main control program runs at dSpace MicroLabBox

[1] Soft-Land^{TM} by SMAC Corporation, `https://www.smac-mca.com/technical-resources/programmability-soft-land`.

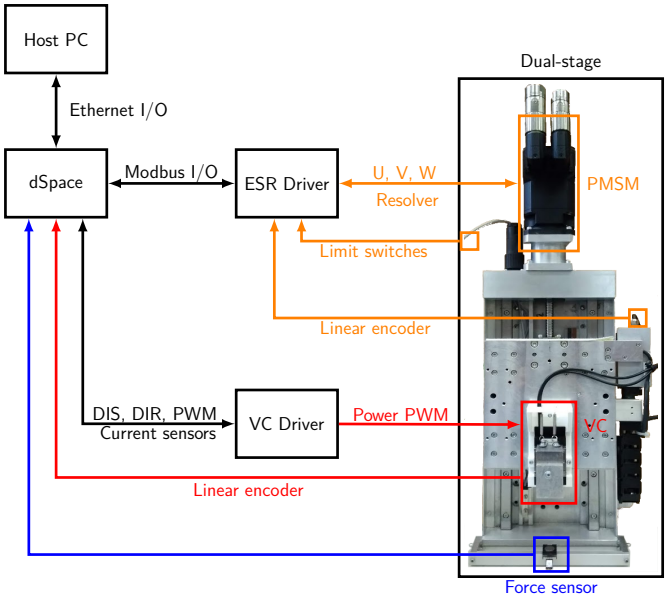

Fig. 1. Experimental platform as used with the proposed control algorithm

platform, which sends position setpoints to the ESR driver and provides analog/digital interface for the VC driver electronics. For the reference industrial solution, a different setup is used. Instead of dSpace, we send the trajectory setpoints directly from the PC to the ESR driver. The VC driver is the SMAC control unit in this case. The Soft-Land routine is implemented using a macro language of the manufacturer, uploaded to the control unit, and initiated using a command over the RS232 bus. The force sensor Honeywell FSAGPD at the bottom of the platform serves only for verification purposes, it is not used for feedback control.

3. MATHEMATICAL MODEL

3.1 Hybrid model

We have modeled the dual-stage system as a hybrid system with three modes. The first mode M_1 describes the free motion with no contact. The second mode M_2 models the limit position of the VC motor. Finally, the third mode M_3 models the contact of the end effector with the environment (wafer with components). In the figure 2, we can see the schematic of the mode M_1. There are two inputs to the system, primary stage velocity v_1, and secondary stage force F_2. Since we use the PMSM motor with a control unit in the velocity mode, we modeled the velocity directly as an input. In reality, the velocity has a trapezoidal character, as is the standard in the industry, but transitions are negligible for our purposes. Mode M_2 has the same structure as M_1, only the parameters of the spring k_2 and b_2 are changed to $k_{2\mathrm{lim}}$ and $b_{2\mathrm{lim}}$, respectively. This serves as an easy way how to model the limit position of the secondary stage, which is necessary for simulation of the proposed soft-landing procedure. The contact mode M_3 changes the model structure by introducing the linear Kelvin-Voigt model of the impact in the form of an additional spring k_3 and a damper b_3, as mentioned for example in Flores and Lankarani (2016).

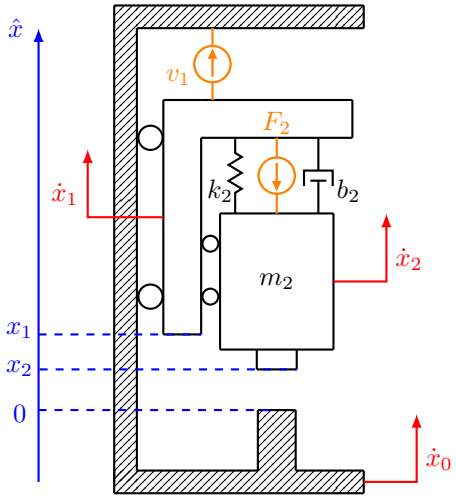

Fig. 2. Mechanical system during free motion (mode M_1)

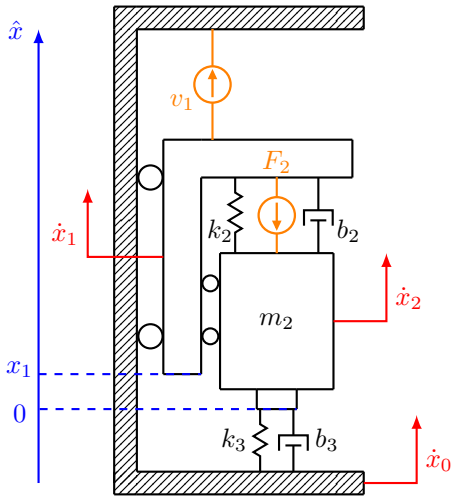

Fig. 3. Mechanical system during contact (mode M_3)

The bond graph representation of the system is displayed in figure 4.

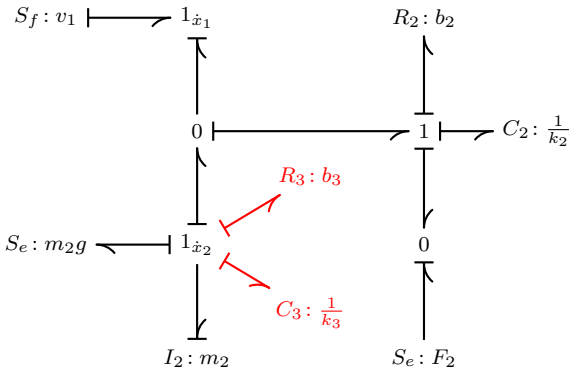

Fig. 4. Bond graph representation of the mechanical system. Additional parameters of the mode M_3 highlighted in red

The resulting equations from the bond graphs for the mode M_1 are as follows:

$$\frac{dx_1}{dt} = v_1, \tag{1}$$

$$\frac{dp_2}{dt} = -m_2 g - b_2\left(\frac{p_2}{m_2} - v_1\right) - q_2 k_2 - F_2, \tag{2}$$

$$\frac{dq_2}{dt} = \frac{p_2}{m_2} - v_1, \tag{3}$$

where x_1 is the primary stage position, p_2 momentum of the end effector and q_2 displacement of the secondary stage spring.

After linearization at the equilibrium of the spring:

$$\begin{bmatrix} \dot{x}_1 \\ \dot{p}_2 \\ \Delta\dot{q}_2 \end{bmatrix} = \begin{bmatrix} 0 & 0 & 0 \\ 0 & -\frac{b}{m_2} & -k_2 \\ 0 & \frac{1}{m_2} & 0 \end{bmatrix} \begin{bmatrix} x_1 \\ p_2 \\ \Delta q_2 \end{bmatrix} + \begin{bmatrix} 1 & 0 \\ b_2 & -k_f \\ -1 & 0 \end{bmatrix} \begin{bmatrix} v_1 \\ i \end{bmatrix}. \tag{4}$$

For the mode M_3, the equations are:

$$\begin{bmatrix} \dot{x}_1 \\ \dot{p}_2 \\ \Delta\dot{q}_2 \\ \dot{q}_3 \end{bmatrix} = \begin{bmatrix} 0 & 0 & 0 & 0 \\ 0 & -\frac{b_2+b_3}{m_2} & -k_2 & -k_3 \\ 0 & \frac{1}{m_2} & 0 & 0 \\ 0 & \frac{1}{m_2} & 0 & 0 \end{bmatrix} \begin{bmatrix} x_1 \\ p_2 \\ \Delta q_2 \\ q_3 \end{bmatrix} + \begin{bmatrix} 1 & 0 \\ b_2 & -k_f \\ -1 & 0 \\ 0 & 0 \end{bmatrix} \begin{bmatrix} v_1 \\ i \end{bmatrix}, \tag{5}$$

where the state q_3 is the displacement of the impact spring. We are also interested in the position of the end effector x_2, which can be computed as $x_2 = x_1 + \Delta q_2$.

3.2 Model Implementation

We implemented the model as a hybrid system in the hybrid system description language (HYSDEL). Using Hybrid Toolbox by Bemporad (2004), the model can be compiled into a Mixed Logical Dynamical (MLD) model and simulated. The switching between the modes M_1, M_2 and M_3 is done by the state automaton (figure 5).

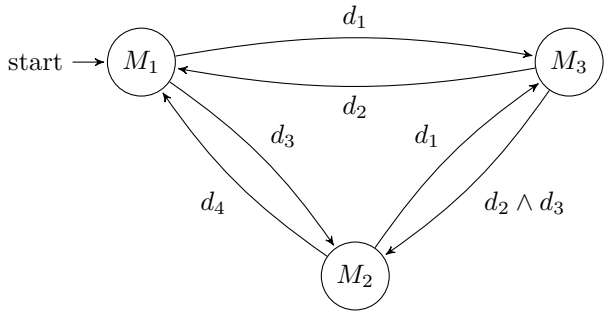

Fig. 5. State automaton of the hybrid system

The logical conditions d_1, d_2, d_3 and d_4 are defined as follows:

$$d_1 = x_2 \leq -\epsilon, \tag{6}$$

$$d_2 = x_2 \geq 0, \tag{7}$$

$$d_3 = \Delta q_2 \leq \Delta q_{2\text{lim}} - \epsilon, \tag{8}$$

$$d_4 = \Delta q_2 \geq \Delta q_{2\text{lim}}, \tag{9}$$

where $\Delta q_{2\text{lim}}$ is the limit position of the secondary stage (VC motor) and ϵ is a very small number (10^{-6})

which introduces hysteresis to the switching conditions for smoother numerical behaviour. The meaning of the parameters used in the mathematical model is summarized together with their numerical values and units in the table 1.

Par.	Unit	Value	Meaning
m_2	Kg	0.426	VC moving mass
b_2	$\mathrm{N\,s\,m^{-1}}$	5.5	VC damping, static friction
k_2	$\mathrm{N\,m^{-1}}$	190	VC spring stiffness
$b_{2\mathrm{lim}}$	$\mathrm{N\,s\,m^{-1}}$	1×10^3	VC limit damping
$k_{2\mathrm{lim}}$	$\mathrm{N\,m^{-1}}$	2×10^4	VC limit stiffness
b_3	$\mathrm{N\,s\,m^{-1}}$	0	Contact env. damping
k_3	$\mathrm{N\,m^{-1}}$	2×10^4	Contact env. stiffness
g	$\mathrm{m\,s^{-2}}$	9.81	Gravitational acceleration
k_f	$\mathrm{AN^{-1}}$	2.7	VC motor constant
v_1	$\mathrm{m\,s^{-1}}$	input	PMSM stage velocity
F_2	N	input	VC actuating force, $F_2 = k_f i$

Table 1. Model parameters

4. CONTROL DESIGN

4.1 Classical approach—segmentation into position, velocity and force regimes

The commonly used procedure in the industry is to decouple the motion of each axis. In the case of a dual-stage soft landing, this means that the initial positioning is done by the primary stage and the soft landing procedure by the secondary stage. A classical industry-ready solution for soft landing problem is the Soft-Land$^{\mathrm{TM}}$ procedure trademarked by the company SMAC, which is the manufacturer of the voice coil motor used in our experimental platform as the secondary stage. The procedure is described by the pseudocode algorithm 1.

In our setup, the secondary stage is supported by a spring, which changes the behaviour of the linear motion by introducing an additional position-dependent force. The Soft-Land$^{\mathrm{TM}}$ procedure does not count with the presence of a spring, it rather assumes that a motor strong enough to hold the entire mass of the end effector by itself is used. The presence of the spring results in dependence of the steady-state value of the contact force on the impact position. This means that it is possible to tune the input parameter F of the algorithm 1 in a way, that the contact force satisfies given constraints, but in the presence of any deviation from the nominal impact position, it changes notably.

Algorithm 1 Soft-Land$^{\mathrm{TM}}$ by SMAC (single-stage)

procedure SoftLand(F, v)
  Set control unit to velocity feedback loop
  $F_{\max} \leftarrow F$
  $v_{\mathrm{ref}} \leftarrow v$
  Start motion
  while true **do**
    $x_{\mathrm{exp}} \leftarrow v_{\mathrm{ref}} \cdot t$
    $e_x \leftarrow |x_{\mathrm{exp}} - x_{\mathrm{act}}|$
    if $e_x > e_{\mathrm{thr}}$ **then**
      Detect impact
      break
  Push with force $F_{\max}$

4.2 Improvement of the classical approach for a system with a spring

To resolve this problem, we can introduce spring compensation into the Soft-Land$^{\mathrm{TM}}$ algorithm (Algorithm 2). We can do this by re-setting the maximum force every sample. The new maximal force is a sum of the spring compensation force in the particular position and the force we want to push with during the contact.

This improved soft landing procedure is now robust towards the contact position deviation.

Algorithm 2 Soft landing for spring-mass system (single-stage)

procedure SoftLandingSpring(F, v, k)
  Set control unit to velocity feedback loop
  $F_{\max} \leftarrow F$
  $v_{\mathrm{ref}} \leftarrow v$
  Start motion
  while true **do**
    $F_{\mathrm{spring}} \leftarrow x_{act} \cdot k$
    $F_{\max} \leftarrow F_{\mathrm{spring}} + F$
    $x_{\mathrm{exp}} \leftarrow v_{\mathrm{ref}} \cdot t$
    $e_x \leftarrow |x_{\mathrm{exp}} - x_{\mathrm{act}}|$
    if $e_x > e_{\mathrm{thr}}$ **then**
      Detect impact
      break
  Push with force $F_{\max}$

4.3 Dual-stage approach

In the classical approach, the stages are used sequentially in a decoupled manner - first moves the primary, then the secondary stage. The switch between the two motions usually happens after the primary stage signals that the position setpoint is reached and stops. This inherently means that the velocity of the end-effector reaches zero for a short time and the overall duration of the procedure increases.

Our proposed procedure improves this by using both the primary and the secondary stage in parallel by decoupling them in terms of the functionality - the primary takes care of the entire positioning and the secondary is used to regulate the contact force. This solution is based on a reaction force observer (RFOB) (Murakami et al. (1993)), which estimates the force acting on the VC motor. The estimate is then subtracted from the motor force reference, as depicted in the figure 6, by which we essentially compensate the forces acting on the motor by adjusting the force exerted by the motor. By setting the reference force F_{ref}, we can now control the contact force. The disturbance d in the figure 6 symbolizes in our case the force exerted by contact dynamics.

The reaction force is estimated using the following expression:

$$\hat{F} = \frac{g_{\mathrm{rfob}}}{s + g_{\mathrm{rfob}}} \left(k_f i_{\mathrm{ref}} + kx - b\dot{x} + \frac{g_v}{s + g_v} b\dot{x} \right), \qquad (10)$$

which can be rearranged to the following form:

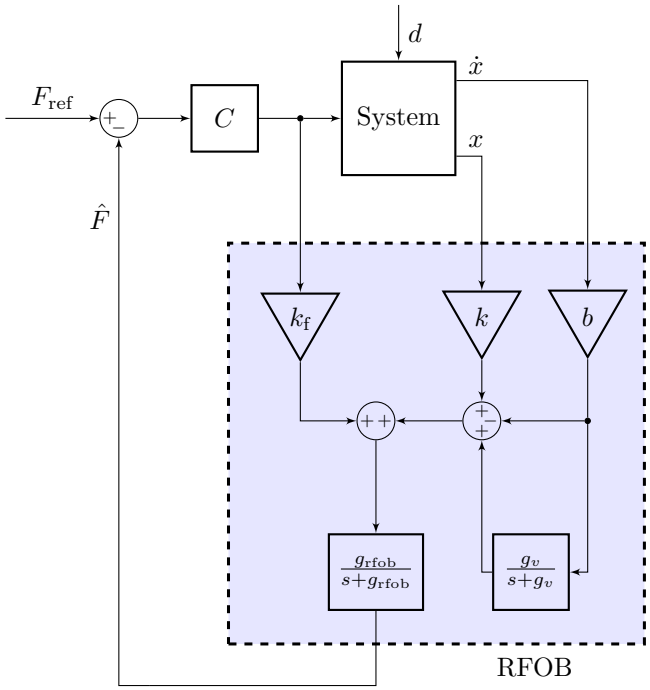

Fig. 6. Reaction force observer (RFOB)

$$\hat{F} = \underbrace{\frac{g_{\text{rfob}}}{s+g_{\text{rfob}}}}_{\text{Low-pass filter}} (k_f i_{\text{ref}} + kx) - \underbrace{\frac{g_{\text{rfob}} s}{(s+g_{\text{rfob}})(s+g_v)}}_{\text{Band-pass filter}} b\dot{x}. \tag{11}$$

The low-pass filter filters the unwanted high frequencies from the estimate. The band-pass filter in addition filters the frequencies around zero from the velocity measurement. This is a practical necessity which results from the nature of our application, as will be explained.

By using the velocity measurement in the RFOB, we are able to set the damping for the motion by the coefficient b. This improves greatly the contact force transition during the impact. With the $b = 0$, the secondary stage behaves as a falling mass, and rebounds can occur during the impact. When the parameter b is increased enough, the rebounds are eliminated. However, during the reciprocal motion, the contact force is increased because of the nonzero DC value of the velocity, which is not the desired behavior. This can be solved by subtracting the low frequencies from the velocity measurement, effectively creating a band-pass filter for the velocity, as shown in equations (10)–(11).

In simulations and experiments, we used a hand-tuned PI controller for the force control (C in the figure 6), which provides satisfactory results.

5. SIMULATIONS

Simulations have been carried out using the hybrid model implementation from the section 3.2. All simulation files are available for free download at *Matlab Central* repository [2] .

[2] `https://www.mathworks.com/matlabcentral/fileexchange/73393-simulation-of-dual-stage-soft-landing`

The simulations show clearly that the characteristics of the contact force during impact and reciprocal stage motion can be improved by setting the damping parameter b. In figure 7, we can see that in a case when b matches the spring damping exactly, the resulting contact force has an oscillatory behaviour. When we increase the b, the oscillations are successfully damped, but the force does not follow the reference during the reciprocal motion of the linear stages, because of the nonzero DC value of the velocity measurement. This is improved significantly by subtracting the low frequencies from the velocity measurement, i.e. creating a high pass filter, or rather a bandpass filter when combined with the output low pass filter.

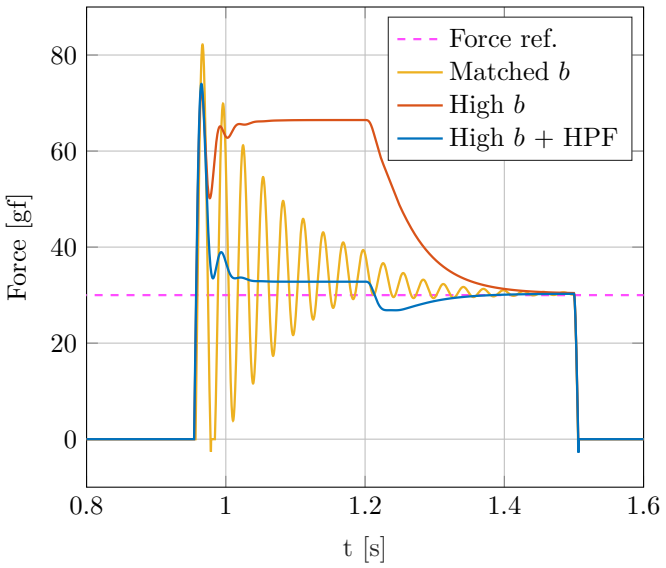

Fig. 7. Contact force dependence on the RFOB damping b, simulation results

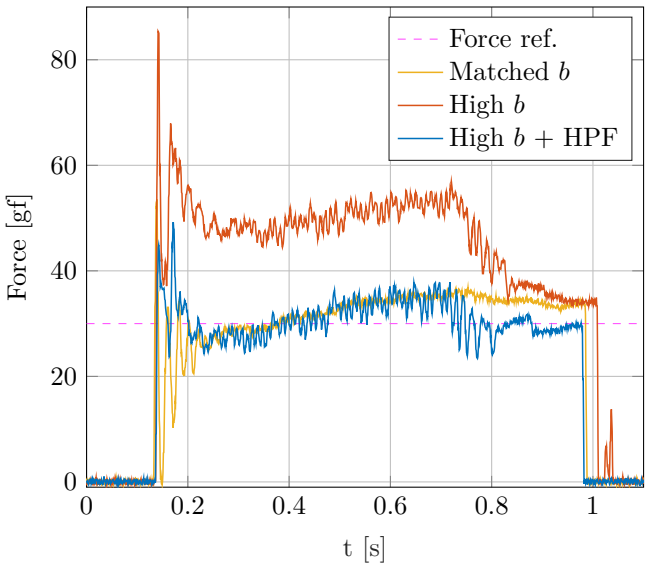

Fig. 8. Contact force dependance on the RFOB damping b, experimental results

6. EXPERIMENTS

6.1 Contact force and RFOB

The experiments from the simulation have been conducted on the experimental platform as well, the results are shown in figure 8. In comparison to the simulation, the data match fairly well, given the simple linear impact model. It is apparent that the matched damping causes rebounds and oscillatory behavior during impact, while high damping causes tracking problems during reciprocal motion and even rebounds during the restitution. The proposed method with a bandpass velocity filter has shown better performance in both the simulation and the experiment.

6.2 Soft landing benchmark

In the soft landing experiments, both the reference procedure and our proposed procedure were tuned to the limits of the experimental platform. Since the resulting time is dependent on several factors, the algorithms had to be tuned with an emphasis on equality of conditions for both procedures. This means for example that the range in which we expect the impact to happen and therefore the impact velocity is reached is the same in both cases. In both procedures a maximal contact velocity has been chosen such that the impact impulse almost reaches the upper constraint, but still satisfies it.

The benchmark test for the procedures is to start 20 mm above the impact position and achieve the impact as fast as possible, while keeping the constraints on the contact force. For die soldering, it is important not to cross a certain maximum force during the procedure, since it could potentially damage the component. At the same time, the contact force should not fall below a certain value as well, for the soldering to succeed. These constraints are not standardized and can differ with the size of the manipulated component. For the benchmark, we have chosen that the acceptable interval for the contact force is from 20 gf to 40 gf. The goal is to keep the contact force within the constraints for a time period of approximately 500 ms, which is the time needed for successful soldering.

The results for the reference procedure are displayed on figures 9 and 11, for our proposed procedure on figures 10 and 12. The results show clearly, that the proposed soft landing procedure offers a possible slight time improvement at the price of the contact force oscillations during the reciprocal motion of the stages. However, as long as the contact force stays within the constraints, we do not care about the oscillations from a technological perspective.

The experiments have shown that the proposed dual-stage approach offers a slight time improvement as a trade-off for slightly less steady contact force when compared to the conventional approach. In applications where the requirements on the steadiness of the contact force are not too strict, this could be beneficial, since even a tenth of a second per cycle could mean a noticeable difference in long term operational/production periods. The experiments are documented in the form of a short video available at `https://youtu.be/BBQp_Mypqao`.

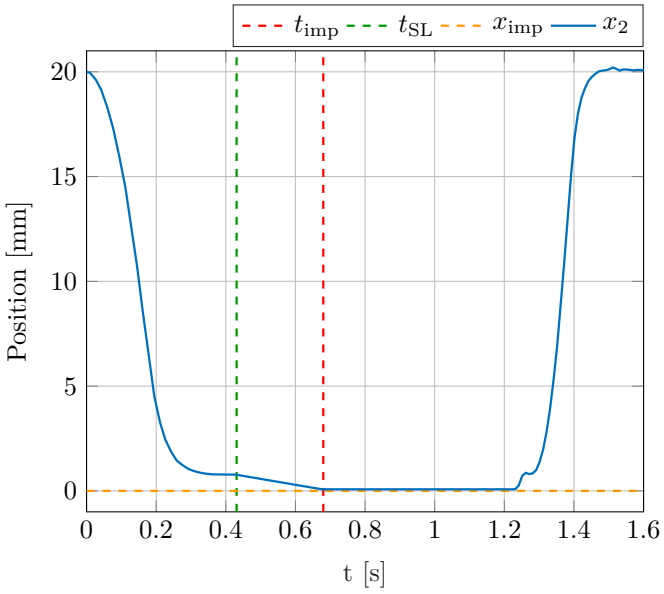

Fig. 9. Reference procedure, trajectory of the end effector coordinate x_2. The Soft-Land routine starts at time t_{SL}. The end effector impacts the wafer at time t_{imp}. The impact position is labeled as $x_{\text{imp}} = 0$.

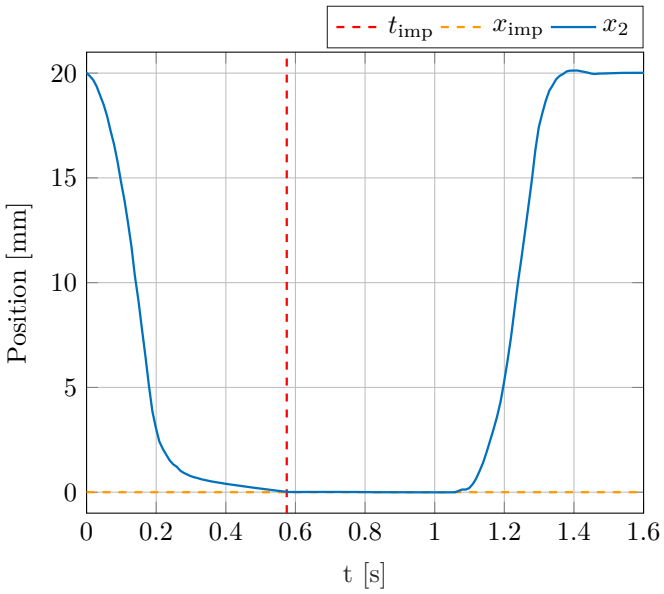

Fig. 10. Proposed dual-stage soft landing procedure, trajectory of the end effector coordinate x_2.

7. CONCLUSION

In this paper we described a practical control design problem of *soft landing* for a *dual-stage* configuration. We proposed a systematic solution based on the concept of *reaction force observer* (RFOB). We compared it with an intuitive extension of a documented simple method implemented in commercial drivers. The comparison was done using both simulations and laboratory experiments. The experiments were also documented with a video. Although the motivation for solving this problem was very concrete and practical—pick-and-place manipulators in the semiconductor industry—we kept the exposition

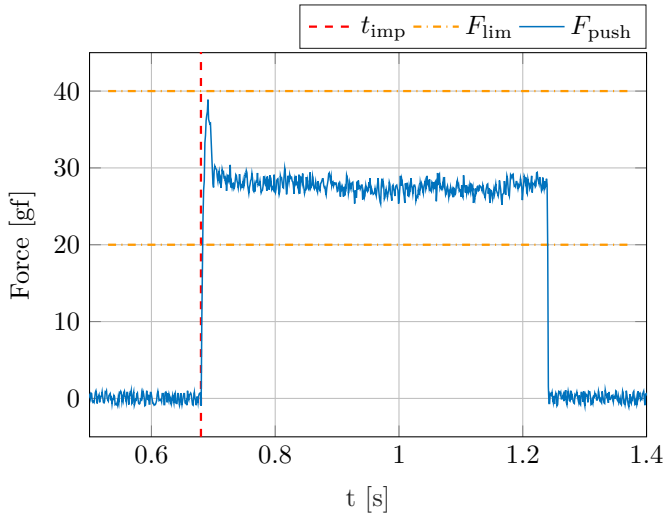

Fig. 11. Reference procedure, contact force F_{push}. Time axis is zoomed to the contact phase and corresponds to the figure 9.

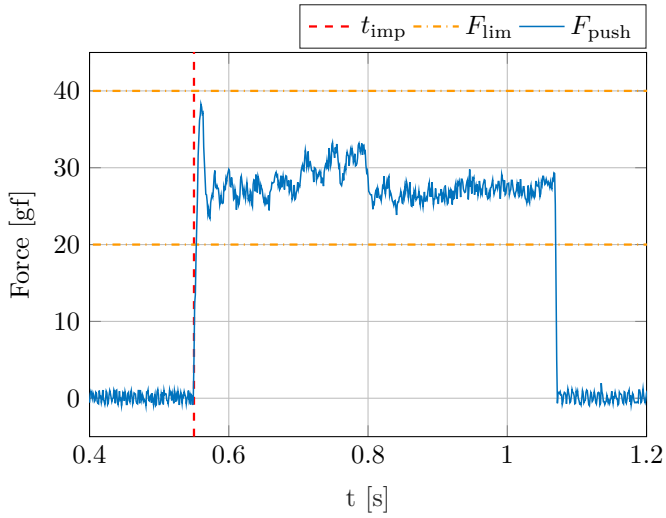

Fig. 12. Proposed procedure, contact force F_{push}. Time axis is zoomed to the contact phase and corresponds to the figure 10.

general enough so that both practitioners who need to solve a similar problem and researchers who want to find a benchmark could benefit from the paper. We even strengthened the reproducibility of the presented research by sharing the Simulink model and Matlab codes through a public repository.

ACKNOWLEDGEMENTS

We acknowledge help with setting up the PMSM control loops and Modbus communication from Lukáš Černý. The authors would also like to thank Krištof Pučejdl, Loi Do, and other members of the AA4CC research group for their assistance.

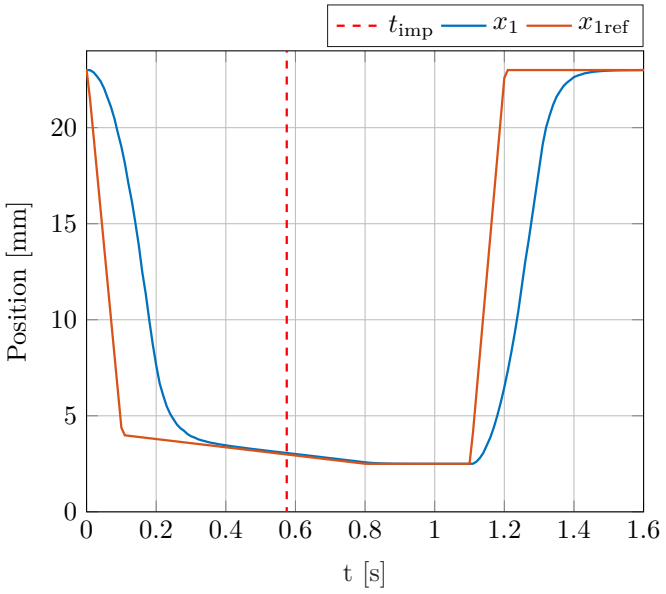

Fig. 13. Position reference and the actual position of the primary axis during the proposed procedure. The stages perform a reciprocal movement from the the impact at t_{imp} to $t = 0.8\,\text{s}$. Resulting contact force is on the figure 12.

REFERENCES

Bemporad, A. (2004). Hybrid Toolbox - User's Guide. `http://cse.lab.imtlucca.it/~bemporad/hybrid/toolbox`.

Clayton, G.M., Dudley, C.J., and Leang, K.K. (2014). Range-based control of dual-stage nanopositioning systems. *Review of Scientific Instruments*, 85(4), 045003. doi:10.1063/1.4870903.

Řezáč, M. and Hurák, Z. (2013). Structured MIMO design for dual-stage inertial stabilization: Case study for HIFOO and Hinfstruct solvers. *Mechatronics*, 23(8), 1084–1093. doi:10.1016/j.mechatronics.2013.08.003.

Flores, P. and Lankarani, H.M. (2016). *Contact Force Models for Multibody Dynamics*. Springer, New York, NY, 1 edition.

Katsura, S., Matsumoto, Y., and Ohnishi, K. (2006). Analysis and experimental validation of force bandwidth for force control. *IEEE Transactions on Industrial Electronics*, 53(3), 922–928. doi:10.1109/TIE.2006.874262.

Murakami, T., Yu, F., and Ohnishi, K. (1993). Torque sensorless control in multidegree-of-freedom manipulator. *IEEE Transactions on Industrial Electronics*, 40(2), 259–265. doi:10.1109/41.222648.

Peng, B., Quan, J., Yin, Z., and Xiong, Y. (2010). The analysis and control of pick-and-place process in flip-chip. In *2010 2nd International Conference on Mechanical and Electronics Engineering*, volume 1, V1–404–V1–408. doi:10.1109/ICMEE.2010.5558519.

Raibert, M.H. and Craig, J.J. (1981). Hybrid Position/Force Control of Manipulators. *Journal of Dynamic Systems, Measurement, and Control*, 103(2), 126–133. doi:10.1115/1.3139652.

Sariyildiz, E. and Ohnishi, K. (2015). An Adaptive Reaction Force Observer Design. *IEEE/ASME Transactions on Mechatronics*, 20(2), 750–760. doi:10.1109/TMECH.2014.2321014.